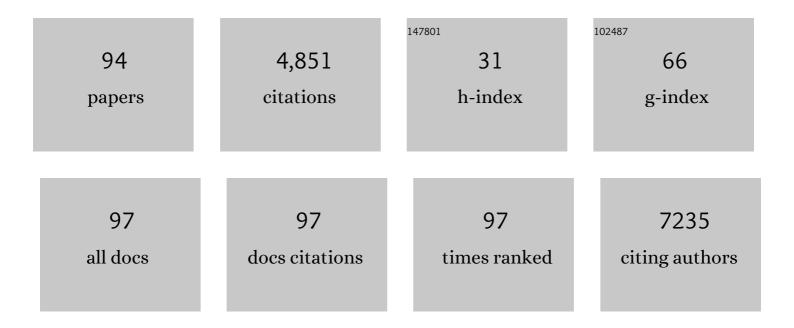
Harini Veeraraghavan

List of Publications by Year in descending order

Source: https://exaly.com/author-pdf/4337118/publications.pdf Version: 2024-02-01



#	Article	lF	CITATIONS
1	Heterogeneous Tumor-Immune Microenvironments among Differentially Growing Metastases in an Ovarian Cancer Patient. Cell, 2017, 170, 927-938.e20.	28.9	368
2	Haralick texture analysis of prostate MRI: utility for differentiating non-cancerous prostate from prostate cancer and differentiating prostate cancers with different Gleason scores. European Radiology, 2015, 25, 2840-2850.	4.5	322
3	Automatic classification of prostate cancer Gleason scores from multiparametric magnetic resonance images. Proceedings of the National Academy of Sciences of the United States of America, 2015, 112, E6265-73.	7.1	322
4	A rectal cancer organoid platform to study individual responses to chemoradiation. Nature Medicine, 2019, 25, 1607-1614.	30.7	320
5	Vision 20/20: Perspectives on automated image segmentation for radiotherapy. Medical Physics, 2014, 41, 050902.	3.0	262
6	MR Imaging of Rectal Cancer: Radiomics Analysis to Assess Treatment Response after Neoadjuvant Therapy. Radiology, 2018, 287, 833-843.	7.3	257
7	Unravelling tumour heterogeneity using next-generation imaging: radiomics, radiogenomics, and habitat imaging. Clinical Radiology, 2017, 72, 3-10.	1.1	244
8	GBM Volumetry using the 3D Slicer Medical Image Computing Platform. Scientific Reports, 2013, 3, 1364.	3.3	185
9	Multiple Resolution Residually Connected Feature Streams for Automatic Lung Tumor Segmentation From CT Images. IEEE Transactions on Medical Imaging, 2019, 38, 134-144.	8.9	176
10	Autosegmentation for thoracic radiation treatment planning: A grand challenge at AAPM 2017. Medical Physics, 2018, 45, 4568-4581.	3.0	169
11	Computer vision algorithms for intersection monitoring. IEEE Transactions on Intelligent Transportation Systems, 2003, 4, 78-89.	8.0	148
12	Differentiation of Uterine Leiomyosarcoma from Atypical Leiomyoma: Diagnostic Accuracy of Qualitative MR Imaging Features and Feasibility of Texture Analysis. European Radiology, 2017, 27, 2903-2915.	4.5	128
13	Breast cancer subtype intertumor heterogeneity: MRIâ€based features predict results of a genomic assay. Journal of Magnetic Resonance Imaging, 2015, 42, 1398-1406.	3.4	119
14	Breast cancer molecular subtype classifier that incorporates MRI features. Journal of Magnetic Resonance Imaging, 2016, 44, 122-129.	3.4	114
15	Technical Note: Extension of CERR for computational radiomics: A comprehensive MATLAB platform for reproducible radiomics research. Medical Physics, 2018, 45, 3713-3720.	3.0	114
16	Tumor-Aware, Adversarial Domain Adaptation from CT to MRI for Lung Cancer Segmentation. Lecture Notes in Computer Science, 2018, 11071, 777-785.	1.3	104
17	A novel representation of inter-site tumour heterogeneity from pre-treatment computed tomography textures classifies ovarian cancers by clinical outcome. European Radiology, 2017, 27, 3991-4001.	4.5	92
18	Deep learning-based auto-segmentation of targets and organs-at-risk for magnetic resonance imaging only planning of prostate radiotherapy. Physics and Imaging in Radiation Oncology, 2019, 12, 80-86.	2.9	82

HARINI VEERARAGHAVAN

#	Article	IF	CITATIONS
19	Multimodal data integration using machine learning improves risk stratification of high-grade serous ovarian cancer. Nature Cancer, 2022, 3, 723-733.	13.2	82
20	Impact of image preprocessing on the scanner dependence of multi-parametric MRI radiomic features and covariate shift in multi-institutional glioblastoma datasets. Physics in Medicine and Biology, 2019, 64, 165011.	3.0	79
21	Patchâ€based generative adversarial neural network models for head and neck MRâ€only planning. Medical Physics, 2020, 47, 626-642.	3.0	67
22	A machine learning model that classifies breast cancer pathologic complete response on MRI post-neoadjuvant chemotherapy. Breast Cancer Research, 2020, 22, 57.	5.0	63
23	Association between CT-texture-derived tumor heterogeneity, outcomes, and BRCA mutation status in patients with high-grade serous ovarian cancer. Abdominal Radiology, 2019, 44, 2040-2047.	2.1	50
24	Clinical utility of radiomics at baseline rectal MRI to predict complete response of rectal cancer after chemoradiation therapy. Abdominal Radiology, 2020, 45, 3608-3617.	2.1	45
25	Crossâ€modality (CTâ€MRI) prior augmented deep learning for robust lung tumor segmentation from small MR datasets. Medical Physics, 2019, 46, 4392-4404.	3.0	42
26	MRI radiomic features are associated with survival in melanoma brain metastases treated with immune checkpoint inhibitors. Neuro-Oncology, 2019, 21, 1578-1586.	1.2	42
27	Reliability of tumor segmentation in glioblastoma: Impact on the robustness of MRIâ€radiomic features. Medical Physics, 2019, 46, 3582-3591.	3.0	38
28	Radiogenomics of rectal adenocarcinoma in the era of precision medicine: A pilot study of associations between qualitative and quantitative MRI imaging features and genetic mutations. European Journal of Radiology, 2019, 113, 174-181.	2.6	38
29	Classifiers for driver activity monitoring. Transportation Research Part C: Emerging Technologies, 2007, 15, 51-67.	7.6	36
30	Preoperative MRI-radiomics features improve prediction of survival in glioblastoma patients over MGMT methylation status alone. Oncotarget, 2019, 10, 660-672.	1.8	35
31	Machine learning-based prediction of microsatellite instability and high tumor mutation burden from contrast-enhanced computed tomography in endometrial cancers. Scientific Reports, 2020, 10, 17769.	3.3	35
32	Multiatlas approach with local registration goodness weighting for MRI-based electron density mapping of head and neck anatomy. Medical Physics, 2017, 44, 3706-3717.	3.0	32
33	Robust target detection and tracking through integration of motion, color, and geometry. Computer Vision and Image Understanding, 2006, 103, 121-138.	4.7	30
34	The distance discordance metric—a novel approach to quantifying spatial uncertainties in intra- and inter-patient deformable image registration. Physics in Medicine and Biology, 2014, 59, 733-746.	3.0	30
35	Head and neck cancer patient images for determining autoâ€segmentation accuracy in T2â€weighted magnetic resonance imaging through expert manual segmentations. Medical Physics, 2020, 47, 2317-2322.	3.0	29
36	Segmenting lung tumors on longitudinal imaging studies via a patient-specific adaptive convolutional neural network. Radiotherapy and Oncology, 2019, 131, 101-107.	0.6	27

#	Article	IF	CITATIONS
37	PSIGAN: Joint Probabilistic Segmentation and Image Distribution Matching for Unpaired Cross-Modality Adaptation-Based MRI Segmentation. IEEE Transactions on Medical Imaging, 2020, 39, 4071-4084.	8.9	27
38	Appearance Constrained Semi-Automatic Segmentation from DCE-MRI is Reproducible and Feasible for Breast Cancer Radiomics: A Feasibility Study. Scientific Reports, 2018, 8, 4838.	3.3	26
39	Integration of proteomics with CT-based qualitative and radiomic features in high-grade serous ovarian cancer patients: an exploratory analysis. European Radiology, 2020, 30, 4306-4316.	4.5	25
40	Integrated Multi-Tumor Radio-Genomic Marker of Outcomes in Patients with High Serous Ovarian Carcinoma. Cancers, 2020, 12, 3403.	3.7	24
41	Learning to Recognize Video-Based Spatiotemporal Events. IEEE Transactions on Intelligent Transportation Systems, 2009, 10, 628-638.	8.0	23
42	Volumetric analysis of IDH-mutant lower-grade glioma: a natural history study of tumor growth rates before and after treatment. Neuro-Oncology, 2020, 22, 1822-1830.	1.2	23
43	Automatic segmentation of brain metastases using T1 magnetic resonance and computed tomography images. Physics in Medicine and Biology, 2021, 66, 175014.	3.0	21
44	Inter- and intrafraction motion assessment and accumulated dose quantification of upper gastrointestinal organs during magnetic resonance-guided ablative radiation therapy of pancreas patients. Physics and Imaging in Radiation Oncology, 2022, 21, 54-61.	2.9	21
45	Active learning guided interactions for consistent image segmentation with reduced user interactions. , 2011, 2011, 1645-1648.		18
46	Performance Evaluation of a Multi-Robot Search & Retrieval System: Experiences with MinDART. Journal of Intelligent and Robotic Systems: Theory and Applications, 2008, 52, 363-387.	3.4	17
47	Computed Tomography–Derived Radiomic Metrics Can Identify Responders to Immunotherapy in Ovarian Cancer. JCO Precision Oncology, 2019, 3, 1-13.	3.0	16
48	No fear: University of Minnesota Robotics Day Camp introduces local youth to hands-on technologies. , 0, , .		15
49	Library of deep-learning image segmentation and outcomes model-implementations. Physica Medica, 2020, 73, 190-196.	0.7	15
50	CT images with expert manual contours of thoracic cancer for benchmarking autoâ€segmentation accuracy. Medical Physics, 2020, 47, 3250-3255.	3.0	15
51	Communication Strategies in Multi-robot Search and Retrieval: Experiences with MinDART. , 2007, , 317-326.		15
52	Driver activity monitoring through supervised and unsupervised learning. , 0, , .		14
53	Unified Cross-Modality Feature Disentangler for Unsupervised Multi-domain MRI Abdomen Organs Segmentation. Lecture Notes in Computer Science, 2020, 12262, 347-358.	1.3	14
54	Combining multiple tracking modalities for vehicle tracking at traffic intersections. , 2004, , .		13

#	Article	IF	CITATIONS
55	Switching Kalman Filter-Based Approach for Tracking and Event Detection at Traffic Intersections. , 0, , \cdot		13
56	Learning Dynamic Event Descriptions in Image Sequences. , 2007, , .		13
57	Prospectively-validated deep learning model for segmenting swallowing and chewing structures in CT. Physics in Medicine and Biology, 2022, 67, 024001.	3.0	13
58	Using Robots to Raise Interest in Technology Among Underrepresented Groups. IEEE Robotics and Automation Magazine, 2007, 14, 73-81.	2.0	12
59	Deep learning auto-segmentation and automated treatment planning for trismus risk reduction in head and neck cancer radiotherapy. Physics and Imaging in Radiation Oncology, 2021, 19, 96-101.	2.9	11
60	Simultaneous segmentation and iterative registration method for computing ADC with reduced artifacts from DWâ€MRI. Medical Physics, 2015, 42, 2249-2260.	3.0	10
61	Dynamic multiatlas selectionâ€based consensus segmentation of head and neck structures from CT images. Medical Physics, 2019, 46, 5612-5622.	3.0	10
62	Unpaired Cross-Modality Educed Distillation (CMEDL) for Medical Image Segmentation. IEEE Transactions on Medical Imaging, 2022, 41, 1057-1068.	8.9	10
63	Deep crossâ€modality (MR T) educed distillation learning for cone beam CT lung tumor segmentation. Medical Physics, 2021, 48, 3702-3713.	3.0	9
64	Self-derived organ attention for unpaired CT-MRI deep domain adaptation based MRI segmentation. Physics in Medicine and Biology, 2020, 65, 205001.	3.0	9
65	Combined artificial intelligence and radiologist model for predicting rectal cancer treatment response from magnetic resonance imaging: an external validation study. Abdominal Radiology, 2022, 47, 2770-2782.	2.1	9
66	Learning task specific plans through sound and visually interpretable demonstrations. , 2008, , .		8
67	Nested block selfâ€attention multiple resolution residual network for multiorgan segmentation from CT. Medical Physics, 2022, 49, 5244-5257.	3.0	8
68	Faceted Visualization of Three Dimensional Neuroanatomy By Combining Ontology with Faceted Search. Neuroinformatics, 2014, 12, 245-259.	2.8	6
69	Radiomic Analysis to Predict Histopathologically Confirmed Pseudoprogression in Glioblastoma Patients. Advances in Radiation Oncology, 2023, 8, 100916.	1.2	6
70	Deep Learning-Based Model for Identifying Tumors in Endoscopic Images From Patients With Locally Advanced Rectal Cancer Treated With Total Neoadjuvant Therapy. Diseases of the Colon and Rectum, 2023, 66, 383-391.	1.3	6
71	Adaptive geometric templates for feature matching. , 0, , .		4
72	A multiple-image-based method to evaluate the performance of deformable image registration in the pelvis. Physics in Medicine and Biology, 2016, 61, 6172-6180.	3.0	4

#	Article	IF	CITATIONS
73	TH-A-WAB-06: Joint Segmentation and Sequential Registration Based Approach for Computing Artifact-Free ADC Maps From Multiple DWI-MRI Sequences in Liver. Medical Physics, 2013, 40, 521-521.	3.0	3
74	SU‣â€Jâ€253: The Radiomics Toolbox in the Computational Environment for Radiological Research (CERR). Medical Physics, 2015, 42, 3324-3324.	3.0	3
75	TU-AB-BRA-09: Radiomics and Radiogenomics for Breast Cancer Using Magnetic Resonance Imaging. Medical Physics, 2015, 42, 3588-3588.	3.0	3
76	SU-F-303-16: Multi-Atlas and Learning Based Segmentation of Head and Neck Normal Structures From Multi-Parametric MRI. Medical Physics, 2015, 42, 3541-3541.	3.0	2
77	Real-time tracking for managing suburban intersections. , 0, , .		1
78	Automatic detection and tracking of longitudinal changes of multiple bone metastases from dual energy CT. , 2016, 2016, 168-171.		1
79	Automated Breast Density Measurements From Chest Computed Tomography Scans. Journal of Medical Systems, 2019, 43, 242.	3.6	1
80	Reproducibility of radiomic features using network analysis and its application in Wasserstein k-means clustering. Journal of Medical Imaging, 2021, 8, 031904.	1.5	1
81	TH-C-WAB-01: BEST IN PHYSICS (JOINT IMAGING-THERAPY)-Semi-Automated Probabilistic Segmentation of Head and Neck Anatomy Through Structure Specific Feature Selection From Multi-Sequence MRI. Medical Physics, 2013, 40, 536-536.	3.0	1
82	SU-E-J-64: Landmark and ROI-Enhancement-Assisted Inter-Patient Deformable Registration of 3D Bladder CT Images. Medical Physics, 2013, 40, 164-164.	3.0	1
83	Learning Task Specific Web Services Compositions with Loops and Conditional Branches from Example Executions. , 2010, , .		0
84	Deep learning from small labeled datasets applied to medical image analysis. , 2021, , 279-291.		0
85	Automatic Bone and Marrow Extraction from Dual Energy CT through SVM Margin-Based Multi-Material Decomposition Model Selection. Lecture Notes in Computer Science, 2014, , 149-156.	1.3	Ο
86	SU-E-J-95: A Novel Objective Approach to Identify Scan Outliers in Deformable Image Registration for Longitudinal Datasets. Medical Physics, 2015, 42, 3286-3286.	3.0	0
87	SU‣â€Jâ€255: Automatic Segmentation Refined, Multiple Sliceâ€Wise Voting Based Classification of Tumors From MRI. Medical Physics, 2015, 42, 3325-3325.	3.0	0
88	TUâ€Gâ€⊋04â€02: Automatic Sclerotic Bone Metastases Detection in the Pelvic Region From Dual Energy CT. Medical Physics, 2015, 42, 3633-3633.	3.0	0
89	SUâ€Eâ€Jâ€213: Visualization of Scans and Metrics for Longitudinal Informatics. Medical Physics, 2015, 42, 3314-3314.	3.0	0
90	MO-A-207B-01: Radiomics: Segmentation & Feature Extraction Techniques. Medical Physics, 2016, 43, 3694-3694.	3.0	0

#	Article	IF	CITATIONS
91	TU-AB-BRA-03: Atlas-Based Algorithms with Local Registration-Goodness Weighting for MRI-Driven Electron Density Mapping. Medical Physics, 2016, 43, 3733-3733.	3.0	0
92	MO-A-207B-00: Segmentation & Feature Extraction Techniques. Medical Physics, 2016, 43, 3694-3694.	3.0	0
93	WE-H-BRC-07: Validation of a Commercial Atlas Based Auto-Segmentation Package For Automated Contour Quality Control. Medical Physics, 2016, 43, 3841-3841.	3.0	0
94	Abstract B09: Heterogeneous fates of metastatic lesions linked to immune escape in an ovarian cancer patient. , 2017, , .		0